Journal of Environmental Management 313 (2022) 115000

Contents lists available at ScienceDirect

Journal of Environmental Management

journal homepage: www.elsevier.com/locate/jenvman

Exploring the type and strength of nonlinearity in water quality responses to nutrient loading reduction in shallow eutrophic water bodies: Insights from a large number of numerical simulations

Han Su[a,b], Rui Zou[b,*], Xiaoling Zhang[b], Zhongyao Liang[c], Rui Ye[d], Yong Liu[e,**]

[a] Multidisciplinary Water Management Group, Faculty of Engineering Technology, University of Twente, Enschede, 7500AE, the Netherlands
[b] Rays Computational Intelligence Lab, Beijing Inteliway Environmental Ltd., Beijing, 100085, China
[c] Department of Ecosystem Science and Management, Pennsylvania State University, State College, PA, 16803, USA
[d] Nanjing Smart Water Co. Ltd, Nanjing, 210012, China
[e] State Environmental Protection Key Laboratory of All Materials Flux in Rivers, College of Environmental Science and Engineering, Peking University, Beijing, 100871, China

ARTICLE INFO

Keywords:
Nonlinearity
Water quality
Load reduction
EFDC
Machine learning

ABSTRACT

Reducing the load of nutrients is essential to improve water quality while water quality may not respond to the load reduction in a linear way. Despite nonlinear water quality responses being widely mentioned by studies, there is a lack of comprehensive assessment on the extent and type of nonlinear responses considering the seasonal changes. This study aimed to measure the strength of nonlinearity of theoretically possible water quality responses and explore their potential types in shallow eutrophic water bodies. Hereto, we generated 14,710 numerical water body cases that describe the water quality processes using the Environmental Fluid Dynamics Code (EFDC) and applied eight load reduction scenarios on each water body case. Inflows are simplified from Lake Dianchi. The climate conditions consider three cases: Lake Dianchi, Wissahickon Creek, and Famosa Slough. We then developed a nonlinearity strength indicator to quantify the strength and frequency of nonlinear water quality responses. Based on the quantification of nonlinearity, we clustered all the samples of water quality responses using K-Means, an unsupervised Machine Learning algorithm, to find the potential types of nonlinear water quality responses for TN (total nitrogen), TP (total phosphorus), and Chla (chlorophyll *a*). Results show linear or near-linear response types account for 90%, 69%, and 20% of TN, TP, and Chla samples respectively. TP and Chla could perform more types of nonlinearity. Representative nonlinear water quality responses include disproportional improvement, peak change (disappear, move forwards or afterward), and seasonal deterioration of TN after load reduction. This study would contribute to the current understanding of nonlinear water quality responses to load reduction and provide a basis to study under which conditions the nonlinear responses may emerge.

1. Introduction

The modern human lifestyle has largely changed the local and global nitrogen and phosphorus flows which then lead to severe water quality problems worldwide (Rockström et al., 2009). The changes in nitrogen and phosphorus flows can be attributed to diffuse pollution from agriculture, emissions from industry, and domestic wastewater (Bouwman et al., 2009; Zimmerman et al., 2008). When the exceeding amount of nitrogen and phosphorus flow into water bodies, it results in water quality deterioration threatening drinking water security and the aquatic ecosystem (Smith, 2003). To deal with unprecedented water quality challenges, Sustainable Development Goals (SDGs) include water quality as an explicit target in SDG 6 (clean water and sanitation) and aim to improve water quality by reducing pollution including

* Corresponding author. Rays Computational Intelligence Lab, Beijing Inteliway Environmental Ltd., Huayuandonglu Road No. 30 Building No. 5-5306, Haidian District, Beijing, 100085, China.
** Corresponding author. State Environmental Protection Key Laboratory of All Materials Flux in Rivers, College of Environmental Science and Engineering, Peking University, Beijing, 100871, China.
E-mail addresses: rz5q2008@gmail.com (R. Zou), yongliu@pku.edu.cn (Y. Liu).

https://doi.org/10.1016/j.jenvman.2022.115000
Received 1 December 2021; Received in revised form 7 March 2022; Accepted 28 March 2022
Available online 4 April 2022
0301-4797/

halving the proportion of untreated water by 2030 (ESCAP, 2015).

Reductions in load may not necessarily lead to equivalent water quality improvement, especially for chlorophyll *a* (Chla) (cf. Kemp et al. (2005)). The water quality responses to watershed nutrient loading reduction may be nonlinear. Here, we take the "nonlinear" water quality response as that the load reduction does not proportionally lead to water quality improvement. In another word, one percent of load reduction does not result in one percent of or equivalent water quality improvement. One example of nonlinearity under this definition could be found in the Spokane River and Lake Spokane systems (Zhang et al., 2018). The nonlinearity of water quality responses may result from nonlinear limnological processes, linear processes as well as the randomness of natural processes (Kemp et al., 2009; Larned and Schallenberg, 2018).

The nonlinear responses of water quality could happen in two stages. First, total nitrogen (TN) and total phosphorus (TP) load reduction from the watershed may not lead to linear decreases in TN and TP concentrations of water bodies (Chou et al., 2007; Liu et al., 2009). Second, the decreases in TN and TP concentrations of water bodies could have a "sigma" shape relationship with Chla (McCauley et al., 1989; Prairie et al., 1989; Quinlan et al., 2020; Yuan and Jones, 2020). Chla may change rapidly after TN or TP reach certain concentrations (Quinlan et al., 2020). Because the growth of algae consumes TN and TP in water bodies and the death of algae release TN and TP into water bodies, overall, water quality indicators, like TN, TP, and Chla may respond to load reduction nonlinearly. These nonlinear water quality responses become more complicated when we consider the whole limnological processes including bottom water oxygen and nutrient recycling and benthic primary production (cf. Kemp et al. (2005)).

Current studies focus on the nonlinearity of water quality responses related to eutrophication recovery trajectories. In this case, nonlinearity means and usually is classified according to the existence of hysteresis, bifurcation, and threshold in the stressor (nutrient loading)-response (water quality) relationship (Kemp et al., 2009; Larned and Schallenberg, 2018). Studying the nonlinearity of the eutrophication recovery trajectories require data on both how nutrient loading leads to eutrophication and how nutrient loading reduction leads to water quality improvement. The strength of this nonlinearity could be measured by the adjusted correlation coefficient (Janssen et al., 2017). The interest of hysteresis, bifurcation and threshold could always be tracked back the regime shift of lakes (Scheffer et al., 2001; Scheffer and Carpenter, 2003). Thus, the nonlinearity of eutrophication recovery trajectories concerns more about regime shift rather than dynamics of water quality especially seasonal responses, e.g., Chla peak (Janssen et al., 2017), after nutrient loading reduction. Studies on eutrophication recovery trajectories are seen as part of stressor-response relationships in the aquatic ecosystem. Hunsicker et al. (2016) reviewed the type and strength of nonlinear stressor-response relationships of one of the best studies aquatic ecosystem. They classified the stressor-response relationships as five types according to the curve shape and measured the strength of nonlinearity using the effective degrees of freedom from the generalized additive model. During their review, only a few studies on nutrient loading reduction and water quality were found but the found strength of nonlinearity is high (McQuatters-Gollop et al., 2007). Again, the dynamics of water quality especially seasonal responses after nutrient loading reduction were not explicitly considered in the stressor-response relationship analysis.

Unpacking the type and strength of nonlinearity in water quality responses especially seasonal responses to nutrient loading reduction could bridge the studies on limnological processes and water quality management into a more direct way. On the one hand, knowing the types and strength of nonlinear water quality responses could facilitate further studies on certain limnological processes that may play key roles in understanding when and how the nonlinear responses happen. These key limnological processes are leverage points for eutrophication management. On the other hand, knowing the types and strength of nonlinear water quality responses may prepare decision-makers for any spurious ineffectiveness of pollution controls at the initial stage without losing confidence to take further actions to overcome the dynamically nonlinear complexity.

To consider the seasonal changes of nonlinearity and get more insights on how strong the nonlinearity would be, and what type of nonlinearity may exist, this study designed intensive numerical model experiments combined with an unsupervised machine learning algorithm to detect and classify the theoretically possible nonlinear water quality responses. The experimental models were established based on a state-of-art numerical model that represents key chemical and biological processes in water bodies using boundary conditions simplified from real cases. We ran and assessed the water quality response under different lack characteristics and reduction scenarios. We developed an indicator to detect the nonlinear water quality responses. All the simulations were clustered based on the strength and frequency of nonlinearity to induct the types of nonlinear response and explore the mechanism behind each type via representative samples from simulations.

2. Material and methods

We first established a virtual lake, whose size, initial conditions were fixed during experiments. The inflow inputs of the virtual lake were simplified from real cases. We generated 14,710 water body cases from the virtual lake based on 16 parameters that feature one water body's response to load reduction. We then simulated each water body case under eight nutrient loading reduction scenarios. The time-dependent strength of these theoretically possible nonlinearities in the water quality responses to load reduction was measured. We finally clustered water quality responses samples based on the strength and explored the type of nonlinearity according to representative samples.

2.1. Water quality model preparation

All of our simulations were based on EFDC (Environmental Fluid Dynamics Code) (Hamrick, 1992). EFDC is one of the state-of-art water quality models which have been applied and validated across countries (Bai et al., 2022; Burigato Costa et al., 2019). It is also recommended by US EPA for the use of Total Maximum Daily Loads planning (USEPA, 2018). The water quality processes described by EFDC include physical transportation, atmospheric exchange, adsorption and desorption, algae reaction and absorption, sediment-water flux, and sedimentation (Hamrick, 1996). EFDC includes multiple water quality variables to simulate the response of water quality to load especially when eutrophication may happen. These variables include various forms of nitrogen and phosphorus. We assumed the water quality processes described by EFDC are reliable. If one nonlinearity could be identified from simulations, this nonlinearity could exist in reality since reality is always more complex than models. However, it does not mean the nonlinearity must happen, we take it as theoretically possible.

We established a virtual lake in EFDC. To make it feasible for a large number of numerical simulations, the virtual lake was spatially simplified with one dimension but activated all the water quality processes that are key for eutrophication. This means the spatial effect was not considered in this study. The virtual lake has 2 km width, 2 km length, and 2 m depth. We focused on the response of three water quality indicators: TN, TP, and Chla. The initial water quality condition of the virtual lake is 2.35 mg/L, 0.14 mg/L, and 0.45 μg/L for TN, TP, and Chla respectively. The annual averaged inflow is 3.6 m^3/s. The averaged concentration of TN and TP are 14.12 mg/L and 0.95 mg/L respectively. The inflow conditions were simplified from the EFDC model of Lake Dianchi (Yi et al., 2016).

The meteorological data as well as other EFDC input settings were taken from three EFDC models in previous studies: Lake Dianchi (Yi et al., 2016), Wissahickon Creek (Zou et al., 2010), and Famosa Slough (Chen et al., 2017) (Table 1). This lets us consider the effect of climate on

Table 1
Climate characteristic of the inputs from the three lakes, which were used as input to drive the virtual lake.

Name	Location	Climate	Average temperature (°C)	Average solar short-wave radiation (W/m^2)
Lake Dianchi	Kunming, Yunnan Province, China	Moderate	16.5	155
Wissahickon Creek	Philadelphia, Pennsylvania, USA	Continental	11.4	144
Famosa Slough	City of San Diego, California, USA	Semi-arid	17.2	174

nonlinearity.

2.2. Model experiment design

We fully considered the impact of the characteristic of water bodies and the load reduction strategies. We considered 16 variables in EFDC that affect a water body's response to nutrient loading reduction (Table 2). Within the reasonable range of each variable, we randomly selected a value for each variable to combine these 16 values to generate a water body case.

For each water body case, we operated eight load reduction scenarios where the scenarios were defined by how much (%) TP load is reduced when 1% TN load is reduced. The motivation to design load reduction scenarios in this way is that pollution control may affect the TN/TP ratio in water bodies (Tong et al., 2020). TN/TP ratio is a key factor that could explain nonlinear water quality responses (Prairie et al., 1989). Possible reduced phosphorus when 1% nitrogen is reduced is determined by pollution control infrastructures. We used the ranges of reduced phosphorus from 0.8% to 2.2% according to previous literature reviews on constructed wetlands and wastewater treatment plants (Land et al., 2016; Sayadi et al., 2012). Under each scenario, we simulated four levels of load reduction in addition to the no-reduction case (Table 3).

Combining the 16 variables, we finally generated 14,710 water body cases: 1000 water body cases with the climate conditions from Lake Dianchi, 7356 water body cases with the climate conditions from Wissahickon Creek, and 6354 water body cases with the climate conditions from Famosa Slough. Each water body case was simulated under no reduction boundary conditions and applied eight reduction scenarios. For each scenario, we ran four load reduction levels. In the end, we ran 485,430 (14,710 + 14,710 × 8 × 4) simulations. All the simulations are conducted in three working stations (Intel® Core™ i5-3470 3.20 GHz, RAM 32 GB). The simulations would take around 514 days if all the simulations are run in a single working station. We investigated the three water quality indicators' (TN, TP, and Chla) responses to nutrient loading reduction for the 14,710 water body cases and eight scenarios. Thus, in total, we had 353,040 (14,710 × 8 × 3) samples for analysis.

Table 2
The 16 EFDC variables were sampled to randomly generate water body cases and their respective sampling range.

No.	Variable	Sampling range	Unit
1	Dissolved Organic Nitrogen decay rate	0.01–0.15	d^{-1}
2	Labile Particulate Organic Nitrogen settling rate	0.01–0.15	m/d
3	Base nitrification rate	0.01–0.2	d^{-1}
4	Labile Particulate Organic Phosphorous settling rate	0.1–0.3	m/d
5	Max growth rate of algae group 1	1–3	d^{-1}
6	Max growth rate of algae group 2	1–2.5	d^{-1}
7	Max growth rate of algae group 3	1–2	d^{-1}
8	Basal respiration rate of algae group 1	0.01–0.15	d^{-1}
9	Basal respiration rate of algae group 2	0.01–0.15	d^{-1}
10	Basal respiration rate of algae group 3	0.01–0.15	d^{-1}
11	Settling rate of algae group 1	0.05–0.2	m/d
12	Settling rate of algae group 2	0.15–0.25	m/d
13	Settling rate of algae group 3	0.1–0.2	m/d
14	Dissolved Organic Phosphorous decay rate	0.01–0.15	d^{-1}
15	Labile Particulate Organic Phosphorus hydrolysis	0.01–0.15	d^{-1}
16	Sediment simulation	0 (closed); 1 (open)	–

Table 3
Eight load reduction scenarios and four levels of load reduction that applied to each water body case.

Scenario No.	Reduced TN	0%	10%	20%	30%	40%	Reduced TP load (%)/reduced TN load (%)
1	Reduced	0%	8%	16%	24%	32%	0.8
2	TP	0%	10%	20%	30%	40%	1.0
3		0%	12%	24%	36%	48%	1.2
4		0%	14%	28%	42%	56%	1.4
5		0%	16%	32%	48%	64%	1.6
6		0%	18%	36%	54%	72%	1.8
7		0%	20%	40%	60%	80%	2.0
8		0%	22%	44%	66%	88%	2.2

2.3. Detection of nonlinear water quality responses

We assumed that if water quality responds to load reduction linearly, the improvement of water quality is proportional to the reduced load (Eq. (1)). This equation should hold no matter what time we look into it. Due to the natural seasonal variations, the response may be different across seasons which means the response coefficient has a time dimension (Fig. 1).

$$\Delta WQ_t = A_t \times \Delta L_t \tag{1}$$

Here, ΔL_t is the percentage of load reduction at time t, ΔWQ_t is the percentage of water quality improvement (changes) at time t, and A_t describes the water quality improvement (%) per unit (1%) of load reduction at time t. This equation focuses on continuous load reduction. Here, we measured the water quality responses after the model achieves stability under climate and nutrient loading input conditions.

Sine A_t can be estimated under each reduction level (k), we used a signed standard deviation of $A_{t,k}$ ($sstd_t$) to measure the strength of nonlinearity of water quality response at time t:

$$\mathrm{sstd}_t = \mathrm{sign}\left(mean\left(A_{t,k}\ over\ k\right)\right)\mathrm{std}\left(A_{t,k}\ over\ k\right)\ for\ each\ time\ t \tag{2}$$

If water quality responds to load reduction linearly, then the $A_{t,k}$ across load reduction levels should be the same, which means the $std(A_{t,k})$ is zero. Non-zero $std(A_{t,k})$ indicate a nonlinear water response at time t and the larger $std(A_{t,k})$ indicate a stronger nonlinear response. We also noticed that $A_{t,k}$ could be negative when the water quality indicator becomes higher after reduction (or we named it 'rebound response' for short). However, $std(A_{t,k})$ is always positive. To preserve this information, we used the signed standard deviation of $A_{t,k}$ over k (Fig. 1). To avoid detecting the nonlinear responses caused numerical errors, $sstd_t$ is only calculated on the time t when the water quality indicator is larger than 0.001 under the no-reduction scenario.

2.4. Measuring distances between samples and clustering

To cluster samples of water quality responses, we need to measure pair-wise distances between individual samples: the lower distance indicates water quality responses in two samples are more similar. Here, the distance of two samples is based on the distribution of the $sstd_t$ which describes both the type and frequency of nonlinear responses (Fig. 1). The type of nonlinear responses is suggested by the value of $sstd_t$, e.g., a negative value indicates a higher value of water quality indicator after reduction (rebound response). The frequency of nonlinear responses is suggested by the frequency of far-from-zero $sstd_t$. Since the distribution of $sstd_t$ only depends on the frequency instead of the time when the nonlinear response happens, it makes it possible to conduct a cross-water-body and cross-water-quality-indicator comparison. Specifically, we used the Euclidean distance between the discretized cumulative distribution of $sstd_t$ to measure the distance between samples. We discretized the cumulative distribution on a 0.0025 step from −0.2 to 0.2. The distance used here is similar to the distance used in Kolmogorov–Smirnov test which indicates whether the two distributions are the same or not.

After calculating the distance between samples of water quality responses, we applied K-Means to cluster all the samples to explore the types of nonlinear responses. K-Means is a widely used unsupervised clustering algorithm in Machine Learning (Lloyd, 1982; Sun and Scanlon, 2019). It tries to minimize differences (distances) among simulations belonging to the same types and try to keep the same variances among types. The number of types to be clustered in is a key input parameter for K-Means. To estimate the number of types, we ran K-Means 38 times with the number of types ranging from 2 to 39. The selection of this parameter is based on Elbow Method (Thorndike, 1953). Outputs of K-Means include the type of each simulation and the estimated center of each type.

We selected one representative simulation for each water quality indicator in each type that is closest to the center of the type. We looked into water quality changes in these representative samples to check the representative water quality responses for each type and water quality indicator.

3. Results

3.1. The overall strength of nonlinearity in water quality responses

We got 15 types of nonlinear water quality responses from the 353,040 samples of water quality responses using K-Means. Here, we illustrate all the 15 types based on three dimensions: the percentage of linear ($sstd_t$ <0.01 and >0), nonlinear ($sstd_t$ >0.02), and rebound water quality responses ($sstd_t$ <0) (Fig. 2). Details about the 15 types as well as the representative samples can be found in supplementary materials [Fig. S1 and Table S1], where we show the cumulative distribution of the nonlinearity strength and time series of water quality responses for each type.

The strength of nonlinearity diverse significantly across types. Among the 15 types, type A–D represent linear or near-linear water quality responses. For type A–D, over 90% of the water quality responses are linear ($sstd_t$ <0.01 and >0) or near-linear ($sstd_t$ >0.01 and < 0.02) and the nonlinear responses only account for less than 3% of the simulation time after load reduction ($sstd_t$ <0 or >0.02). Visual checks of these types can hardly identify nonlinear water quality responses, e.g. the shape of time series change. Other types have shown significantly stronger nonlinear responses (type E–K, N–O) and/or rebound nonlinear responses (type L) (Fig. 2), where their linear water quality responses account for less than 80% of the time after load reduction. The spectrum from linear to nonlinear responses seems continuous since the strength of nonlinearity gradually increases across types.

Chla samples generally have stronger nonlinearities than TP, and TP samples have stronger nonlinearities than TN (Fig. 3, details can be

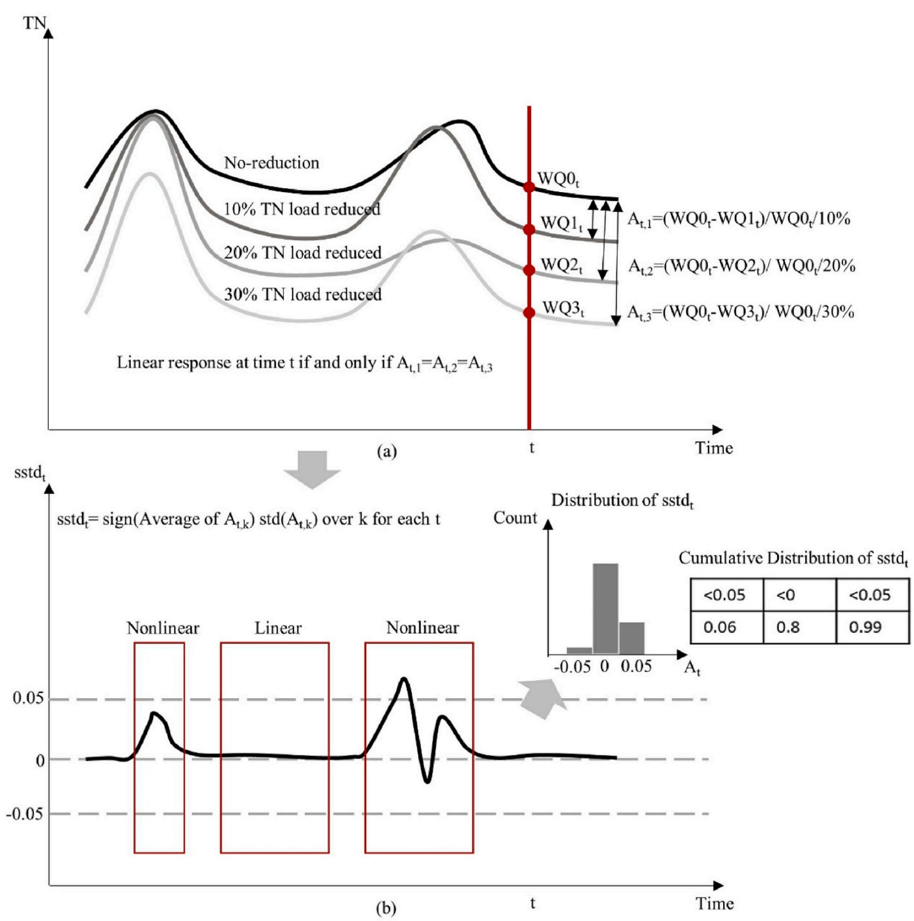

Fig. 1. Detecting nonlinear water quality responses using the distribution of $sstd_t$ (print: can be black and white).

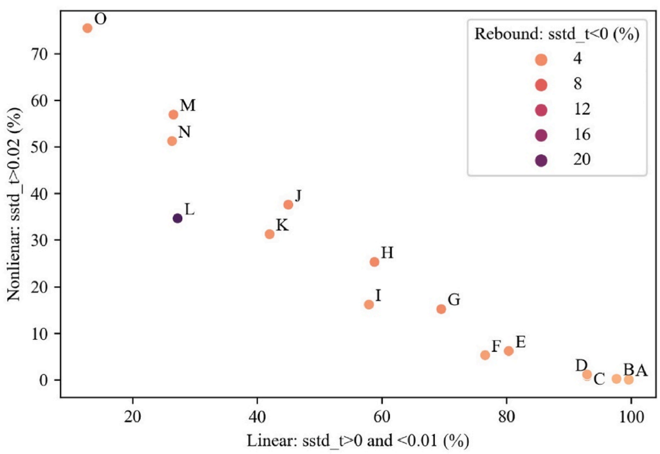

Fig. 2. Characteristics of center sample from each type, featured by the percentage of linear responses ($sstd_t$ <0.01), nonlinear responses ($sstd_t$ >0.02), and rebound nonlinear responses ($sstd_t$ <0) in simulated time after load reduction. Type A–D are taken as linear types, and others are nonlinear. (print: in color). (For interpretation of the references to color in this figure legend, the reader is referred to the Web version of this article.)

found in supplementary materials [Table S1]). From type A to O, the strength of nonlinearity increases, the main contributor to each type changes from TN and TP to TP and Chla, from TP and Chla to Chla. Most samples are clustered into linear types where TN and TP contribute most (type A–D). TP and Chla are the main contributors to nonlinear types. TP and Chla, especially Chla could perform more types of nonlinear responses than TN. Chla has some specific nonlinear types that can hardly be found in TN and TP (type J–O except K).

3.2. The types of nonlinear TN and TP responses

Linear or near-linear water quality responses (type A–D) are the most common types in TN and TP. For TN and TP, 90% and 69% of samples are clustered into the four types. Representative samples of type A–D suggest the pattern of water quality responses does not change along with the changes in load levels (supplementary materials [Table S1]). The shape of the water quality indicator time series remains the same. The nonlinear responses only come from the disproportional improvement of water quality during a limited period. Type E and F are the most two common types of nonlinear responses in TN and TP. Representative TN and TP samples of type E and type F suggest the main difference between the two types is how long the disproportional improvement of water quality lasts. We also observed one exception for TP not belonging to this reason where a TP peak disappears after reduction. This peak only exists for less than 10 days in a no-reduction scenario (Fig. 4). In addition, TP also behaves other four more types of nonlinear responses than TN: type G, H, I, K. Representative samples of the four types indicate the pattern remains the same. The nonlinear water quality responses come from the disproportional improvement of water quality especially when TP changes rapidly.

Other types of nonlinear water quality responses do not take a significant part in our large-scale simulations. Representative samples of TN from these types suggest TN might become higher after reduction. It is only observed at the bottom of the TN time series (Fig. 5). Detailed model inspection suggests that this rebound nonlinearity may relate to the growth of green algae. In these cases, green algae grow sufficiently in high load scenarios and remove TN from the water body by settling. Under low load scenarios, green algae do not have enough nutrients to grow, thus no TN is removed from the water body. Overall, the concentration of TN is higher under low load scenarios than high load scenarios.

3.3. The types of nonlinear Chla responses

Different from TN and TP, nonlinearity dominates Chla's responses to load reduction. The linear and near-linear responses (type A–D) only account for 20% of Chla samples.

Representative examples of the nonlinear types indicate the nonlinearities come from the following four ways (Fig. 6). Firstly, Chla reaches a peak earlier under lower load levels because Chla decreases early. Thus, the changes of Chla are not linear for some time t. Secondly, the disproportional improvement. In addition to the disproportional improvement shown in TN and TP, Chla may only show a marginal improvement at the first level of load reduction but starts to have a much more significant improvement as load reduction levels continue to increase. Most of this kind of disproportional improvement was observed when the concentration of Chla is above 80 μg/L. Third, after a load reduction, Chla reaches a peak earlier in a way of increasing earlier from the bottom. In this case, Chla is always higher than the no-reduction scenario at the peak time. Fourth, the Chla peak may happen later after reduction. In this case, Chla under low-load scenarios would be higher than high-load scenarios because the Chla under high-load scenarios has already undergone decreasing.

4. Discussion

4.1. Potential explanations for nonlinear water quality responses

We believe these nonlinear water quality responses could indicate the key limnological processes on how a water body responds to load reduction. For example, we observed the earlier peak of Chla due to earlier decreases from the top or earlier increases from the bottom. The

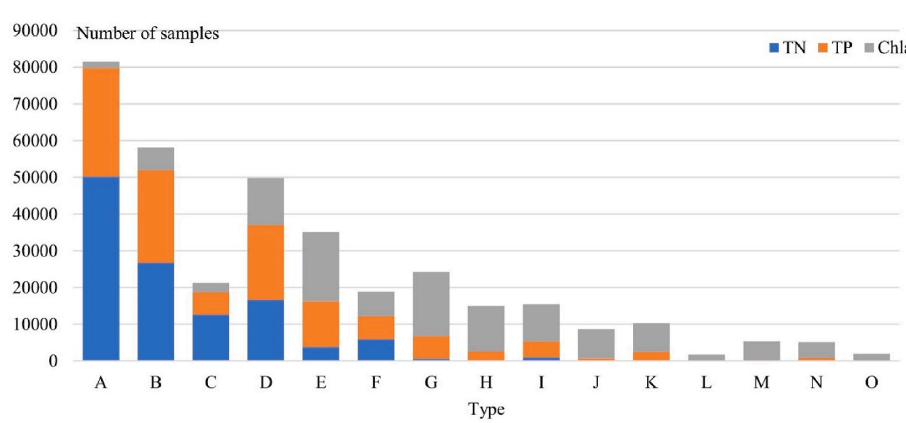

Fig. 3. Clustered water quality response types and the water quality indicators, TN, TP, and Chla. (print: can be black and white).

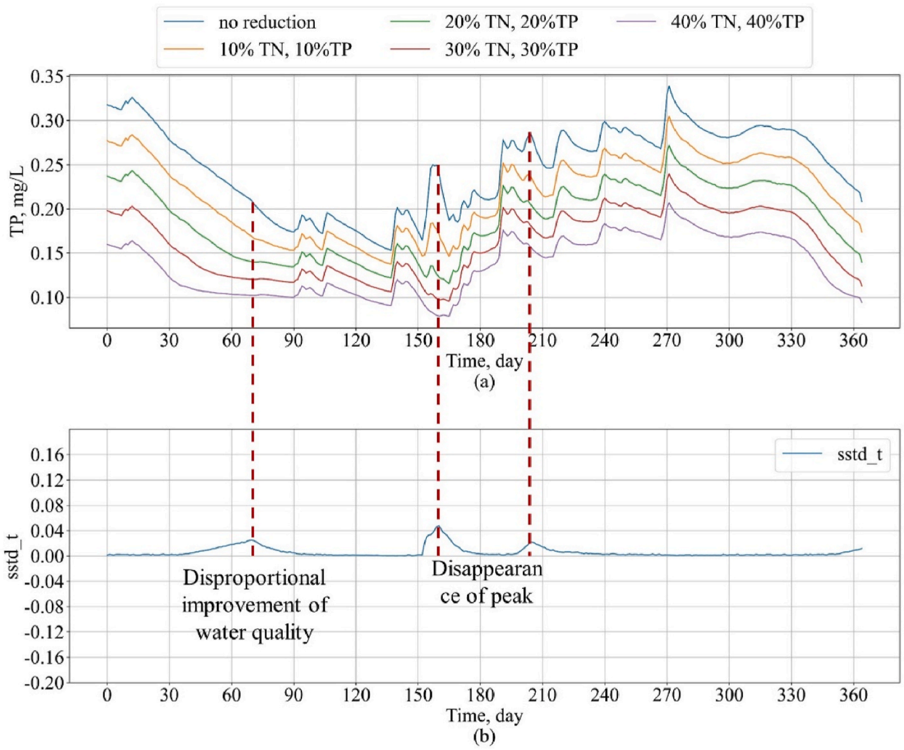

Fig. 4. Representative nonlinear water responses of TP time series (a) and time-dependent nonlinearity strength (b), including the disappearance of peaks and the disproportional changes during rapid increases or decreases. They do not necessarily happen in one single sample simultaneously. Only the Time series of the final year is shown. (print: in color). (For interpretation of the references to color in this figure legend, the reader is referred to the Web version of this article.)

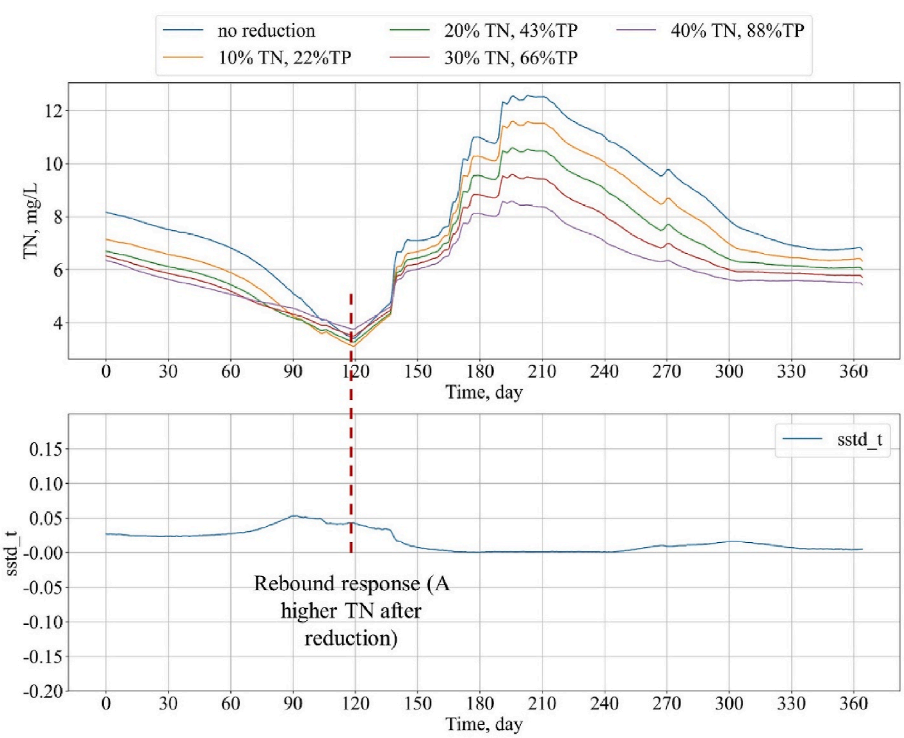

Fig. 5. Rebound nonlinear water responses of TN time series (a) and time-dependent nonlinearity strength (b). Only the Time series of the final year is shown. (print: in color). (For interpretation of the references to color in this figure legend, the reader is referred to the Web version of this article.)

reason behind the earlier decreases from the top may be that after load reduction, nutrition within water bodies is not enough to support the further growth of algae. Thus, Chla decreases earlier than non-reduction scenarios which seem to have an earlier peak. For the earlier peak caused by earlier increases from the bottom, one potential explanation is that reduced load results in lower turbidity and provides a better light

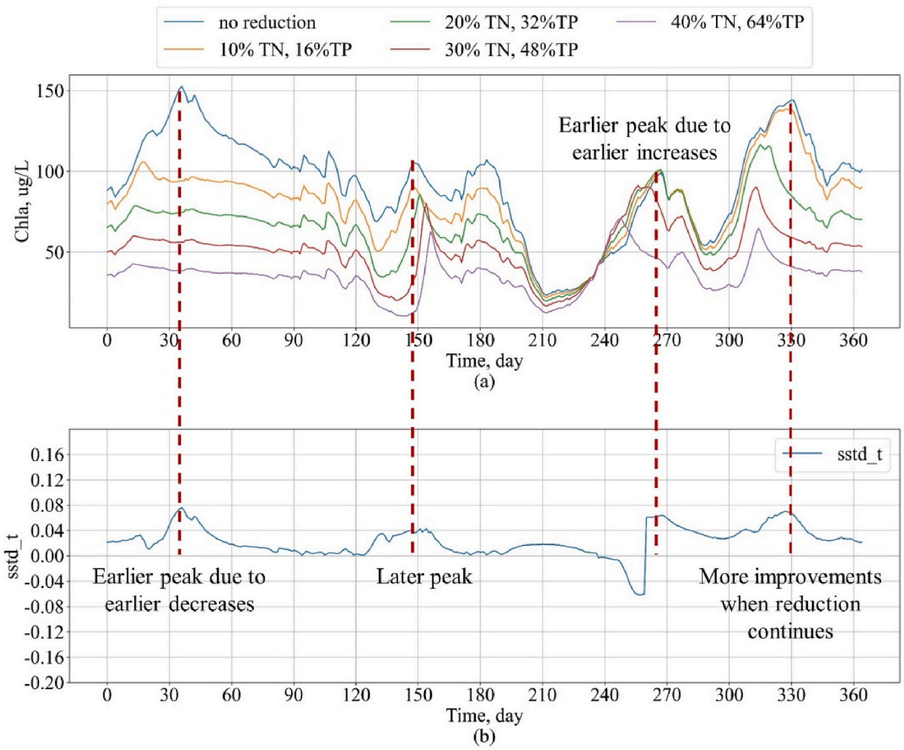

Fig. 6. Four representative nonlinear Chla responses (a) and time-dependent nonlinearity strength (b). They do not necessarily happen in one single sample simultaneously. Only the Time series of the final year is shown. (print: in color). (For interpretation of the references to color in this figure legend, the reader is referred to the Web version of this article.)

condition, allowing the light-limit algae to grow (McQuatters-Gollop et al., 2007).

The dynamics of algal groups may lie behind many nonlinear water quality responses to nutrient loading reduction. In EFDC, three algal groups are simulated: cyanobacteria, diatoms, and green algae. The load reduction may have a distinct impact on them (McQuatters-Gollop et al., 2007; Riemann et al., 2015). Some react linearly while others react nonlinearly. This leads to the changes in the relative abundance of algal groups after nutrient loading reduction and thus results in some complex responses not only for Chla but also for TN and TP whose concentration is affected by the growth, respiration, and settling of algae (McGlathery et al., 2013).

We also compared the percentage of each type under the three climate conditions. There is a higher percentage of nonlinear water quality responses in the case of Wissahickon Creek. A lower temperature may increase nonlinearity because of the longer algae growth cycle (Taylor et al., 2011; Testa et al., 2022).

These explanations are highly context-dependent, depending on the water body characteristics, climate conditions, load reductions (Filstrup et al., 2014; Huszar et al., 2006; Yuan and Jones, 2020). For one type of nonlinear water quality response, there may be multiple possible limnological mechanisms. Understanding in which conditions there may be nonlinear water quality responses and which factors affect the nonlinear responses will be one of the focuses of the following studies.

4.2. Uncertainties

We measured the pair-wise distances between samples based on the discrete distribution of $sstd_t$. The granularity of the discrete distribution impact the distances. The granularity reflects to what extent we want to distinguish the strength and type of nonlinearity. The current granularity is 0.0025, which is small enough to distinguish the type of linear water quality responses (type A-D). Using a lower granularity (a larger value than 0.0025) will result in fewer types from clustering.

During clustering, we selected the number of types for water quality responses based on the Elbow method. The results were not sensitive to the number of clusters except for the representative water quality responses found through representative examples. We repeated our analysis when the number of clusters is changed to 10 and 14. As the number of types decreases, the number of representative examples also decreases. Some of Chla's nonlinear responses are not found when we cluster samples into fewer types. It makes sense since we could get all the Chla's nonlinear responses if we look into samples one by one. Besides this, other conclusions still hold, e.g., nonlinearity changes gradually, TP and Chla have more types and stronger nonlinearity than TN, most TP and TN samples are linear, and Chla samples are mainly nonlinear.

Despite these uncertainties, our conclusions on the strength and type of nonlinear water quality responses to nutrient loading reduction are supported by previous observations. For example, D'Amario et al. (2019) and Janssen et al. (2017) also reported a significant percentage of water quality responses are linear. The disproportional improvement of TN and TP after load reduction was also observed by Riemann et al. (2015), where they also show the nonlinearities are different across seasons. The peak changes of Chla are supported by Taylor et al. (2011) and Testa et al. (2022).

4.3. Limitations

One of the limitations is we detected the nonlinear response under continuous load reduction and after the model has achieved stability under certain boundary conditions, e.g., climate. This kind of definition only lets us focus on the nonlinearity without including time lag. The time lag is an important topic in nonlinear water quality responses studies (Meals et al., 2010; Vero et al., 2018). However, the complexity of time lag and the dependence on real-world context prevents us to include time lag in this study. We acknowledge that lacking consideration of time lag would make it impossible to detect some types of nonlinearity. More types of nonlinear water quality responses are expected when time lag is included.

Model is a kind of simplicity of reality, so EFDC. Some simplifications in EFDC may reduce the strength of nonlinearity. For example, the zooplankton and detritus are not included in the EFDC, which may play a critical role in eutrophic lakes (Arhonditsis et al., 2008; Ger et al., 2014). This means the potential water quality response in the real world may be more complicated than what we illustrated.

Another limitation is the selection of climate conditions, load inputs, and water body characteristics. We got climate conditions from three freshwater bodies, Lake Dianchi, Wissahickon Creek, and Famosa Slough. These three water bodies are located in neither tropical regions nor alpine regions. Water bodies in the tropical or alpine region may respond to load reduction in a different way (Huszar et al., 2006). The availability of climate conditions limits us to look into the water bodies in moderate, continental, arid regions and affected by intensive human activities. Studies also indicate the depth and elevation of the water body, land use of the watershed, and features of nutrient loading also correlate with the type of nonlinear responses of water quality (Filstrup et al., 2014; Yuan and Jones, 2020). More water body cases developed from real cases with different water body characteristics may increase the type of nonlinear responses. Furthermore, the inclusion of spatial context of water bodies may add more nonlinearities (Janssen et al., 2017).

One more limitation is the way we cluster nonlinear water responses. The clustering is mainly based on the distribution of $sstd_t$, i.e. the strength and frequency of nonlinearity. Water quality indicators may have different responses that could result in the same distribution of $sstd_t$. For example, Chla improves fast and then slowly may have the same $sstd_t$ distribution when Chla improves slowly and then fast. The current indicator, $sstd_t$, cannot distinguish the two ways. This means there might be several patterns of water quality responses within one type of nonlinearity found by our study, even though they are similar in terms of the nonlinearity in disproportional water quality improvement.

Despite the limitations, studying nonlinearity using numerical simulations has strengths: it could avoid the impact of randomness from natural processes. Though the climate data was from observations, it can be fixed during simulations, which means we could check how the nonlinearity changes along with water bodies characteristics under the same inflow and climate conditions. It is impossible only based on observations to study the nonlinearity (Larned and Schallenberg, 2018; Testa et al., 2022). Clustering samples based on a large number of simulations is robust to outliers, which may result from randomness. Clustering samples would result in each cluster with a large number of samples. The outliers usually do not affect the cluster. This means we focused on the nonlinearities that may be representative instead of outliers that may be unlikely observed in the real world. The water quality model also allows us to track specific processes that lead to nonlinearity that could be further validated by empirical studies.

5. Conclusions

Understanding how water quality responds to load reduction could facilitate the identification of effective pollution management. This study conducted large-scale numerical simulations to measure the strength of nonlinearity and explore the potential nonlinear water quality responses for TN, TP, and Chla. Among the three water quality indicators, Chla has the highest strength of nonlinearity and TP has the second. TP and Chla, especially for Chla, have shown more types of nonlinearity compared to TN. The potential nonlinear water quality responses include disproportional water quality improvement, peak moves forwards or afterwords, peak disappears. This study contributes to the current understanding of end-to-end relationships between load reduction and water quality responses. Further analysis is needed to better understand on which conditions the nonlinear water quality responses emerge.

CRediT author statement

Han SU: Methodology, Software, Formal analysis, Investigation, Writing - Original Draft, Writing - Review & Editing, Visualization. **Rui ZOU**: Conceptualization, Methodology, Software, Formal analysis, Investigation, Resources, Writing - Review & Editing, Supervision, Project administration, Funding acquisition. **Xiaoling ZHANG**: Formal analysis, Writing - Original Draft, Writing - Review & Editing. **Zhongyao LIANG**: Formal analysis, Writing - Review & Editing. **Rui YE**: Formal analysis, Writing - Review & Editing. **Yong LIU**: Resources, Writing - Review & Editing, Supervision, Funding acquisition.

Declaration of competing interest

The authors declare that they have no known competing financial interests or personal relationships that could have appeared to influence the work reported in this paper.

Acknowledgments

This work was supported by the National Natural Science Foundation of China (51721006, 42142047), Open Fund Project of Yunnan Key Laboratory of Pollution Process and Management of Plateau Lake-Watershed (grant number 2016PL03) and High-performance Computing Platform of Peking University.

Appendix A. Supplementary data

Supplementary data to this article can be found online at https://doi.org/10.1016/j.jenvman.2022.115000.

References

Arhonditsis, G.B., Perhar, G., Zhang, W., Massos, E., Shi, M., Das, A., 2008. Addressing Equifinality and Uncertainty in Eutrophication Models, vol. 44. https://doi.org/10.1029/2007WR005862.

Bai, J., Zhao, J., Zhang, Z., Tian, Z., 2022. Assessment and a review of research on surface water quality modeling. Ecol. Model. 466 https://doi.org/10.1016/j.ecolmodel.2022.109888.

Bouwman, A., Beusen, A.H., Billen, G., 2009. Human alteration of the global nitrogen and phosphorus soil balances for the period 1970–2050. Global Biogeochem. Cycles 23.

Burigato Costa, C.M.S., da Silva Marques, L., Almeida, A.K., Leite, I.R., de Almeida, I.K., 2019. Applicability of water quality models around the world—a review. Environ. Sci. Pollut. Control Ser. 26, 36141–36162. https://doi.org/10.1007/s11356-019-06637-2.

Chen, Y., Zou, R., Han, S., Bai, S., Faizullabhoy, M., Wu, Y., Guo, H., 2017. Development of an integrated water quality and macroalgae simulation model for tidal marsh eutrophication control decision support. Water 9. https://doi.org/10.3390/w9040277.

Chou, W.S., Lee, T.C., Lin, J.Y., Yu, S.L., 2007. Phosphorus load reduction goals for feitsui reservoir watershed, taiwan. Environ. Monit. Assess. 131, 395–408. https://doi.org/10.1007/s10661-006-9485-1.

D'Amario, S.C., Rearick, D.C., Fasching, C., Kembel, S.W., Porter-Goff, E., Spooner, D.E., Williams, C.J., Wilson, H.F., Xenopoulos, M.A., 2019. The prevalence of nonlinearity and detection of ecological breakpoints across a land use gradient in streams. Sci. Rep. 9, 3878. https://doi.org/10.1038/s41598-019-40349-4.

ESCAP, 2015. List of indicator proposals (11 August 2015), reference document for the Monitoring the Sustainable Development Goals: meeting to identify Asia-Pacific regional and sub-regional priorities. Bangkok.

Filstrup, C.T., Wagner, T., Soranno, P.A., Stanley, E.H., Stow, C.A., Webster, K.E., Downing, J.A., 2014. Regional variability among nonlinear chlorophyll-phosphorus relationships in lakes. Limnol. Oceanogr. 59, 1691–1703. https://doi.org/10.4319/lo.2014.59.5.1691.

Ger, K.A., Hansson, L.-A., Lürling, M., 2014. Understanding cyanobacteria-zooplankton interactions in a more eutrophic world, 59, pp. 1783–1798. https://doi.org/10.1111/fwb.12393.

Hamrick, J.M., 1992. A Three-Dimensional Environmental Fluid Dynamics Computer Code: Theoretical and Computational Aspect.

Hamrick, J.M., 1996. User's Manual for the Environmental Fluid Dynamics Computer Code.

Hunsicker, M.E., Kappel, C.V., Selkoe, K.A., Halpern, B.S., Scarborough, C., Mease, L., Amrhein, A., 2016. Characterizing driver-response relationships in marine pelagic ecosystems for improved ocean management. Ecol. Appl. 26, 651–663. https://doi.org/10.1890/14-2200/suppinfo.

Huszar, V.L., Caraco, N.F., Roland, F., Cole, J., 2006. Nutrient-chlorophyll Relationships in Tropical-Subtropical Lakes: Do Temperate Models Fit? Nitrogen Cycling in the Americas: Natural and Anthropogenic Influences and Controls. Springer, pp. 239–250.
Janssen, A.B.G., de Jager, V.C.L., Janse, J.H., Kong, X., Liu, S., Ye, Q., Mooij, W.M., 2017. Spatial identification of critical nutrient loads of large shallow lakes: implications for Lake Taihu (China). Water Res. 119, 276–287. https://doi.org/10.1016/j.watres.2017.04.045.
Kemp, W.M., Boynton, W.R., Adolf, J.E., Boesch, D.F., Boicourt, W.C., Brush, G., Cornwell, J.C., Fisher, T.R., Glibert, P.M., Hagy, J.D., Harding, L.W., Houde, E.D., Kimmel, D.G., Miller, W.D., Newell, R.I.E., Roman, M.R., Smith, E.M., Stevenson, J. C., 2005. Eutrophication of Chesapeake Bay: historical trends and ecological interactions. Mar. Ecol. Prog. Ser. 303, 1–29. https://doi.org/10.3354/meps303001.
Kemp, W.M., Testa, J.M., Conley, D.J., Gilbert, D., Hagy, J.D., 2009. Temporal responses of coastal hypoxia to nutrient loading and physical controls. Biogeosciences 6, 2985–3008. https://doi.org/10.5194/bg-6-2985-2009.
Land, M., Granéli, W., Grimvall, A., Hoffmann, C.C., Mitsch, W.J., Tonderski, K.S., Verhoeven, J.T.A., 2016. How effective are created or restored freshwater wetlands for nitrogen and phosphorus removal? A systematic review. Environ. Evid. 5 https://doi.org/10.1186/s13750-016-0060-0.
Larned, S.T., Schallenberg, M., 2018. Stressor-response relationships and the prospective management of aquatic ecosystems. N. Z. J. Mar. Freshw. Res. 53, 489–512. https://doi.org/10.1080/00288330.2018.1524388.
Liu, W.C., Chen, W.B., Kimura, N., 2009. Impact of phosphorus load reduction on water quality in a stratified reservoir-eutrophication modeling study. Environ. Monit. Assess. 159, 393–406. https://doi.org/10.1007/s10661-008-0637-3.
Lloyd, S., 1982. Least squares quantization in PCM. IEEE Trans. Inf. Theor. 28, 129–137.
McCauley, E., Downing, J.A., Watson, S., 1989. Sigmoid relationships between nutrients and chlorophyll among lakes. Can. J. Fish. Aquat. Sci. 46, 1171–1175.
McGlathery, K.J., Reidenbach, M.A., D'Odorico, P., Fagherazzi, S., Pace, M.L., Porter, J. H., 2013. Nonlinear dynamics and alternative stable states in shallow coastal systems. Oceanography 26, 220–231.
McQuatters-Gollop, A., Raitsos, D.E., Edwards, M., Pradhan, Y., Mee, L.D., Lavender, S.J., Attrill, M.J., 2007. A long-term chlorophyll data set reveals regime shift in North Sea phytoplankton biomass unconnected to nutrient trends. Limnol. Oceanogr. 52, 635–648. https://doi.org/10.4319/lo.2007.52.2.0635.
Meals, D.W., Dressing, S.A., Davenport, T.E., 2010. Lag time in water quality response to best management practices: a review. J. Environ. Qual. 39, 85–96. https://doi.org/10.2134/jeq2009.0108.
Prairie, Y.T., Duarte, C.M., Kalff, J., 1989. Unifying nutrient–chlorophyll relationships in lakes. Can. J. Fish. Aquat. Sci. 46, 1176–1182. https://doi.org/10.1139/f89-153.
Quinlan, R., Filazzola, A., Mahdiyan, O., Shuvo, A., Blagrave, K., Ewins, C., Moslenko, L., Gray, D.K., O'Reilly, C.M., Sharma, S., 2020. Relationships of total phosphorus and chlorophyll in lakes worldwide. Limnol. Oceanogr. 66, 392–404. https://doi.org/10.1002/lno.11611.
Riemann, B., Carstensen, J., Dahl, K., Fossing, H., Hansen, J.W., Jakobsen, H.H., Josefson, A.B., Krause-Jensen, D., Markager, S., Stæhr, P.A., Timmermann, K., Windolf, J., Andersen, J.H., 2015. Recovery of Danish coastal ecosystems after reductions in nutrient loading: a holistic ecosystem Approach. Estuar. Coast 39, 82–97. https://doi.org/10.1007/s12237-015-9980-0.
Rockström, J., Steffen, W., Noone, K., Persson, Å., Chapin III, F.S., Lambin, E., Lenton, T. M., Scheffer, M., Folke, C., Schellnhuber, H.J., Nykvist, B., de Wit, C.A., Hughes, T., van der Leeuw, S., Rodhe, H., Sörlin, S., Snyder, P.K., Costanza, R., Svedin, U., Falkenmark, M., Karlberg, L., Corell, R.W., Fabry, V.J., Hansen, J., Walker, B., Liverman, D., Richardson, K., Crutzen, P., Foley, J., 2009. Planetary boundaries: exploring the safe operating space for humanity. Ecol. Soc. 14 https://doi.org/10.5751/es-03180-140232.
Sayadi, M., Kargar, R., Doosti, M., Salehi, H., 2012. Hybrid constructed wetlands for wastewater treatment: a worldwide review. Proceedings of the international academy of ecology environmental sciences 2, 204.
Scheffer, M., Carpenter, S., Foley, J.A., Folke, C., Walker, B., 2001. Catastrophic shifts in ecosystems. Nature 413, 591–596. https://doi.org/10.1038/35098000.
Scheffer, M., Carpenter, S.R., 2003. Catastrophic regime shifts in ecosystems: linking theory to observation. Trends Ecol. Evol. 18, 648–656. https://doi.org/10.1016/j.tree.2003.09.002.
Smith, V.H., 2003. Eutrophication of freshwater and coastal marine ecosystems a global problem. Environ. Sci. Pollut. Res. 10, 126–139.
Sun, A.Y., Scanlon, B.R., 2019. How can Big Data and machine learning benefit environment and water management: a survey of methods, applications, and future directions. Environ. Res. Lett. 14, 073001.
Taylor, D.I., Oviatt, C.A., Borkman, D.G., 2011. Non-linear responses of a coastal aquatic ecosystem to large decreases in nutrient and organic loadings. Estuar. Coast 34, 745–757. https://doi.org/10.1007/s12237-010-9312-3.
Testa, J.M., Boynton, W.R., Hodgkins, C.L.S., Moore, A.L., Bailey, E.M., Rambo, J., 2022. Biogeochemical states, rates, and exchanges exhibit linear responses to large nutrient load reductions in a shallow, eutrophic urban estuary. Limnol. Oceanogr. https://doi.org/10.1002/lno.12037.
Thorndike, R.L., 1953. Who belongs in the family? Psychometrika 18, 267–276.
Tong, Y., Wang, M., Peñuelas, J., Liu, X., Paerl, H.W., Elser, J.J., Sardans, J., Couture, R.-M., Larssen, T., Hu, H., Dong, X., He, W., Zhang, W., Wang, X., Zhang, Y., Liu, Y., Zeng, S., Kong, X., Janssen, A.B.G., Lin, Y., 2020. Improvement in municipal wastewater treatment alters lake nitrogen to phosphorus ratios in populated regions. Proc. Natl. Acad. Sci. Unit. States Am. 117, 11566–11572. https://doi.org/10.1073/pnas.1920759117.
USEPA, 2018. Overview of Total Maximum Daily Loads (TMDLs). https://www.epa.gov/tmdl/overview-total-maximum-daily-loads-tmdls. (Accessed 7 July 2020).
Vero, S.E., Basu, N.B., Van Meter, K., Richards, K.G., Mellander, P.-E., Healy, M.G., Fenton, O., 2018. The environmental status and implications of the nitrate time lag in Europe and North America. Hydrogeol. J. 26, 7–22.
Yi, X., Zou, R., Guo, H., 2016. Global sensitivity analysis of a three-dimensional nutrients-algae dynamic model for a large shallow lake. Ecol. Model. 327, 74–84. https://doi.org/10.1016/j.ecolmodel.2016.01.005.
Yuan, L.L., Jones, J.R., 2020. Rethinking phosphorus-chlorophyll relationships in lakes. Limnol. Oceanogr. 9999, 1–11. https://doi.org/10.1002/lno.11422.
Zhang, C., Brett, M.T., Brattebo, S.K., Welch, E.B., 2018. How well does the mechanistic water quality model CE-QUAL-W2 represent biogeochemical responses to. Climatic and Hydrologic Forcing? 54, 6609–6624. https://doi.org/10.1029/2018WR022580.
Zimmerman, J.B., Mihelcic, J.R., Smith, James, 2008. Global Stressors on Water Quality and Quantity. ACS Publications.
Zou, R., Liu, Y., Riverson, J., Parker, A., Carter, S., 2010. A nonlinearity interval mapping scheme for efficient waste load allocation simulation-optimization analysis. Water Resour. Res. 46 https://doi.org/10.1029/2009wr008753.